A microtubule-binding Rho-GEF controls cell morphology during convergent extension of *Xenopus laevis*

Kristen M. Kwan* and Marc W. Kirschner†

Department of Systems Biology, Harvard Medical School, Boston, MA 02115, USA
*Present address: Department of Neurobiology and Anatomy, University of Utah, Salt Lake City, UT 84132, USA
†Author for correspondence (e-mail: marc@hms.harvard.edu)

Summary

During *Xenopus* development, convergent extension movements mediated by cell intercalation drive axial elongation. While many genes required for convergent extension have been identified, little is known of regulation of the cytoskeleton during these cell movements. Although microtubules are required for convergent extension, this applies only to initial stages of gastrulation, between stages 10 and 10.5. To examine the cytoskeleton more directly during convergent extension, we visualized actin and microtubules simultaneously in live explants using spinning disk confocal fluorescence microscopy. Microtubule depolymerization by nocodazole inhibits lamellipodial protrusions and cell-cell contact, thereby inhibiting convergent extension. However, neither taxol nor vinblastine, both of which block microtubule dynamics while stabilizing a polymer form of tubulin, inhibits lamellipodia or convergent extension. This suggests an unusual explanation: the mass of polymerized tubulin, not dynamics of the microtubule cytoskeleton, is crucial for convergent extension. Because microtubule depolymerization elicits striking effects on actin-based protrusions, the role of Rho-family GTPases was tested. The effects of nocodazole are partially rescued using dominant negative Rho, Rho-kinase inhibitor, or constitutively active Rac, suggesting that microtubules regulate small GTPases, possibly via a guanine-nucleotide exchange factor. We cloned full-length XLfc, a microtubule-binding Rho-GEF. Nucleotide exchange activity of XLfc is required for nocodazole-mediated inhibition of convergent extension; constitutively active XLfc recapitulates the effects of microtubule depolymerization. Morpholino knockdown of XLfc abrogates the ability of nocodazole to inhibit convergent extension. Therefore, we believe that XLfc is a crucial regulator of cell morphology during convergent extension, and microtubules limit its activity through binding to the lattice.

Key words: Convergent extension, Microtubule, XLfc, *Xenopus*

Introduction

Early vertebrate development depends on the coordination of inductive events and morphogenetic movements, driven by specific cell behaviors, which generate, from the spherical egg, a body axis extended in the anterior-posterior dimension. In *Xenopus*, and probably all chordates, axial elongation is driven via mediolateral intercalation of cells toward the midline, resulting in anterior-posterior extension of the tissue as a whole. This set of movements is known collectively as convergent extension (Gerhart and Keller, 1986; Keller et al., 2000). The cellular processes underlying this behavior are best understood for the convergence of dorsal mesoderm toward the midline in *Xenopus*. During this process, cells establish a polarized morphology with active actin-based lamellipodial protrusions, pointing both toward and away from the midline. These protrusions exert force upon neighboring cells, and inhibition of convergent extension is often correlated with dysregulation of these protrusions. For example, perturbations of non-canonical Wnt signaling that inhibit convergent extension cause either defective or hyperactive protrusive behavior at the cellular level (Wallingford et al., 2000) (K.M.K., unpublished).

While the basis of convergent extension has been extensively addressed by classical observational studies, the molecular mechanisms underlying cell behaviors remain obscure. In particular, little is understood about the regulation and function of actin and microtubules during these cell movements. One striking observation suggesting a role for microtubules in convergent extension is the ability of the microtubule depolymerizing drug nocodazole to block mediolateral cell polarity (Lane and Keller, 1997). Exposure of embryos or explants to nocodazole from stage 10 to 19 (the beginning of gastrulation to the end of neurulation) inhibited convergent extension; however, nocodazole treatment from stage 10.5 to 19 (the first appearance of a fully circular blastopore to the end of neurulation) had no effect on the process. Therefore, the microtubule cytoskeleton appeared to be required for a very brief and specific period of time. After stage 10.5, microtubules appear to be dispensable, although there is little analysis of the cellular effects of microtubule depolymerization.

The effect of nocodazole on convergent extension is unlikely to be due to an effect on the cell cycle, as cell division is completely inhibited in the chordamesoderm during this period, as assayed by phospho-histone H3 staining (Saka and

Smith, 2001). In fact, cell cycle blockade is actually necessary to allow the productive cell-cell contacts integral to convergent extension movements (Leise and Mueller, 2004).

We have followed the microtubule requirement to questions of how cell shape and dynamics change during convergent extension. Using spinning disk confocal microscopy, we have documented the microtubule requirement for actin assembly and dynamics. These studies have led to a surprising function for microtubules as a bulk regulator of Rho-family GTPases through a specific Rho-GEF. These results tie signaling to polymer assembly and indicate a direct role for microtubules in regulating cell polarity.

Materials and methods

Xenopus methods

Xenopus eggs were obtained from *X. laevis* frogs (NASCO or bred in our colony), fertilized in vitro, dejellied in 2% cysteine (pH 7.8), and cultured at 14-18°C in 0.1×Marc's modified Ringer's (MMR) (Peng, 1991). Embryos were staged according to Nieuwkoop and Faber (Nieuwkoop and Faber, 1967). For injection, embryos were placed in 0.1×MMR containing 5% Ficoll and 50 μg/ml gentamycin. Injected embryos were cultured in 0.1×MMR containing 50 μg/ml gentamycin at 14-18°C. For dorsal marginal zone (DMZ) explants, the two dorsal cells of a 4-cell embryo were injected equatorially. All injection amounts reported are per blastomere unless otherwise indicated.

DMZ explants for whole-mount analysis were dissected at stage 10 or 10.5 (as noted) and cultured in 0.5×MMR until stage 19. DMZ explants for confocal microscopy were dissected and cultured in 1×Danilchik's for Amy (DFA) plus bovine serum albumin (BSA) (Marsden and DeSimone, 2003), in chambered coverglasses (VWR) and secured below a separate coverslip using Lubriseal stopcock grease (Thomas Scientific). Chambered coverglasses and coverslips were coated overnight at 4°C with BSA (1% in water). Explants for confocal microscopy were oriented with the inner cells down (toward the objective on an inverted scope) and the epithelium up (away from the objective). Confocal imaging was performed on deep chordamesoderm cells.

Transfection of NIH3T3 cells; immunofluorescence of cells and explants

NIH3T3 cells were grown in DMEM+10% calf serum. Cells were grown to 40-70% confluence for transfection with TransIT-LT1 transfection reagent (Mirus). Transfections were performed according to manufacturer's protocol, using 3-6 μg DNA and 15 μl transfection reagent.

Cells and explants were fixed in methanol, permeabilized in modified Barth's solution (MBS) (Peng, 1991) + 0.1% Triton X-100, and blocked in MBS + 0.1% Triton X-100 + 2% BSA. DM1α (monoclonal antibody to tubulin) was used at 1:1000, followed with appropriate secondary antibody. Explants were dehydrated, cleared in 2:1 benzyl benzoate:benzyl alcohol (BB:BA), and mounted for imaging. As methanol fixation destroys eGFP fluorescence, staining for eGFP-tagged constructs was performed using a polyclonal antibody to eGFP (Abcam 6556, 1:1000), followed with appropriate secondary antibody.

Imaging/image analysis

Confocal images were acquired in the Nikon Imaging Center at Harvard Medical School using a Nikon TE2000U inverted microscope with a Perkin Elmer Ultraview Spinning Disk Confocal Head, Hamamatsu Orca-ER cooled CCD Camera and MetaMorph software (Universal Imaging).

Color images of whole explants and embryos were acquired using a Sony 3CCD Color Camera mounted on a Zeiss Stemi SV11 Stereoscope. Explant elongation was quantitated similar to Tahinci and Symes (2003) by measuring the length of the longest vector of each explant and the width of each explant at the point where the mesoderm extends from the neurectoderm. The length/width ratio was calculated for each explant. All images were acquired and measurements performed using Metamorph software (Universal Imaging). Data were analyzed using analysis of variance (ANOVA) and *P*-values determined using Tukey's method.

RNAs/DNAs

Plasmid DNAs were linearized overnight and purified using the Qiagen PCR Purification Kit. RNAs were synthesized using the mMessage mMachine kit (Ambion) for capped RNA, purified using the Qiagen RNeasy Mini Kit, precipitated in ethanol, and resuspended in RNAse-free water.

Morpholino oligonucleotide experiments

Two morpholinos (GeneTools, LLC) were synthesized. MoXLfc (AGAAGAGGACTCAATCCGAGACATA) is complementary to XLfc and spans –1 to +24 of the coding sequence. MoCon, the control morpholino, is the same sequence as MoXLfc, only reversed (ATACAGAGCCTAACTCAGGAGAAGA). Morpholinos were resuspended and diluted in RNAse-free water.

Wobbled-XLfc (wXLfc) was created by altering as many nucleotides as possible in the sequence recognized by MoXLfc, while preserving the amino acid sequence (MSRIESSS). wXLfc has nine nucleotide changes from wild-type XLfc (ATGTC**AAGA**AT**AGAA**-**AGC**TCATCA; changes in bold). For rescue experiments, embryos were first injected in both cells of 2-cell embryos with morpholino oligonucleotides, and subsequently injected at the 4-cell stage in the marginal zone of the two dorsal cells with wXLfc RNA.

Results

Nocodazole inhibits active lamellipodial protrusions within a specific time period during convergent extension

Previously, Lane and Keller (1997) demonstrated that there is a specific period during which microtubules are required for convergent extension. Verifying these results, treatment of explants with the microtubule depolymerizing drug nocodazole (15 μg/ml) starting at stage 10 inhibited convergent extension, while treatment of explants with nocodazole starting at stage 10.5 had no effect on convergent extension (Fig. 1A,B). In all figures, column graphs display quantitation of length/width ratios of explants pictured just prior. A higher length/width ratio indicates a greater degree of convergent extension movements. The extent of elongation in explants treated with nocodazole at stage 10.5 is significantly greater than in explants treated with nocodazole at stage 10 (*P*<0.01).

To determine the effects of microtubule depolymerization at the cellular level, actin and microtubules were imaged simultaneously in live explants. To visualize the complete microtubule lattice, we utilized eGFP-tau. To visualize the growing ends of microtubules, we utilized eGFP-CLIP-170, a microtubule plus-end binding protein. By co-injection of eGFP-tau (100 pg RNA) or eGFP-CLIP-170 (300 pg RNA) with rhodamine-labeled actin protein (15 ng), we could image either actin and the complete microtubule lattice or actin and microtubule plus-ends in living explants. Injections were targeted to the marginal zone of the two dorsal cells of the 4-cell embryo. At the appropriate stage, DMZ explants were cut,
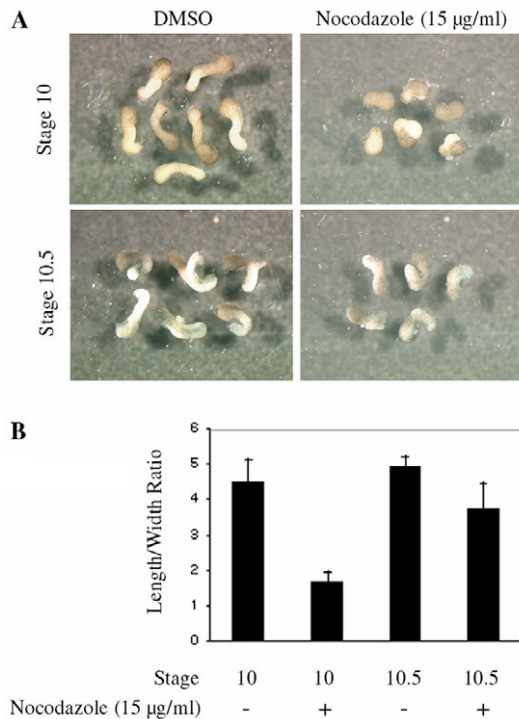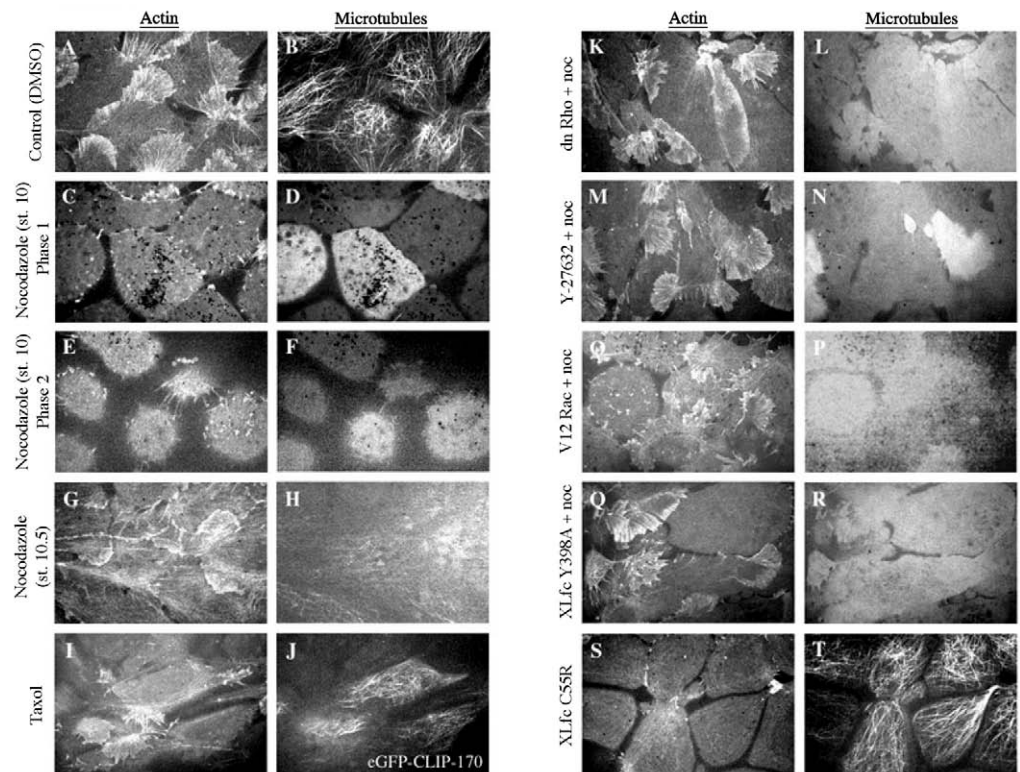
Fig. 1. (A) Nocodazole inhibits convergent extension, but only when explants are treated before stage 10.5. (B) Length/width ratios of explants in (A). Data are from one representative experiment of three trials, analyzing five to eight explants per sample per trial.

secured between coverglasses, and imaged using spinning disk confocal microscopy.

As shown in Fig. 2A, when visualized for rhodamine-actin, cells within the DMZ exhibited one or two large flat lamellipodia extending from one cell to another. The lamellipodia were dynamic, extending and retracting (see Movie 1 in the supplementary material). Using eGFP-tau, the microtubule cytoskeleton is visualized as an extensive network (Fig. 2B), which is also dynamic, as observed by time-lapse confocal microscopy visualizing eGFP-CLIP-170 (Fig. 3A; see Movie 2 in the supplementary material). Within all cells, microtubules can be seen growing and shrinking; the polymers also bend and move (see Movie 3 in the supplementary material).

Nocodazole treatment of cells fully depolymerized the microtubule cytoskeleton, as assayed by fixation and antibody staining for microtubules (Lane and Keller, 1997). Individual microtubules were replaced by diffuse eGFP-tau fluorescence (Fig. 2D,F). Cell morphology and actin-rich protrusions were also affected, in two time-dependent phases. In the first phase, active protrusions were inhibited; many fewer cells produced lamellipodia (Fig. 2C). This became apparent within 15-30 minutes of nocodazole treatment. Prolonged nocodazole treatment produced a second phase of effects: cell-cell contacts are lost and cells look almost dissociated (Fig. 2E). The onset of this phase varied between 1 and 3 hours after initial nocodazole treatment. These effects are unlikely to be due to a pharmacological side effect of nocodazole, as colcemid, a microtubule-depolymerizing drug structurally
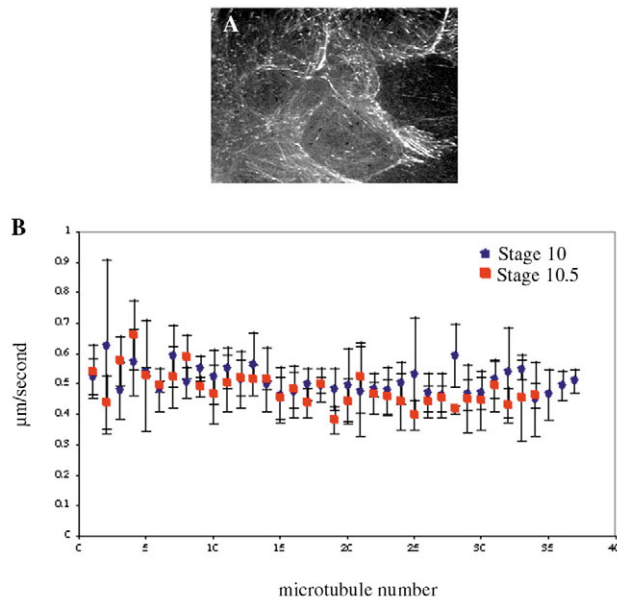
Fig. 2. Confocal microscopic analysis of chordamesoderm explants. (A,C,E,G,I,K,M,O,Q,S) Rhodamine-actin localization. (J) eGFP-CLIP-170 fluorescence. (B,D,F,H,L,N,P,R,T) eGFP-tau fluorescence. (A,B) Control explant. (C,D) Stage 10 explant: nocodazole treatment (15 μg/ml), phase 1. Note loss of lamellipodial protrusions. (E,F) Stage-10 explant: nocodazole treatment (15 μg/ml), phase 2. Note loss of cell-cell contact. (G,H) Stage-10.5 explant: nocodazole treatment (15 μg/ml). Note maintenance of lamellipodia although microtubules are depolymerized. (I,J) Taxol treatment (20 μg/ml) of stage-10 explant. Note maintenance of lamellipodia and stabilized microtubule cytoskeleton, as evidenced by uniform eGFP-CLIP-170 binding. (K,L) dn Rho (200 pg RNA) rescues lamellipodia inhibited by nocodazole (15 μg/ml). (M,N) Y-27632 (10 μmol/l) rescues lamellipodia inhibited by nocodazole (15 μg/ml). (O,P) V12 Rac (25 pg DNA) overcomes the inhibition of lamellipodia by nocodazole (15 μg/ml). (Q,R) XLfc Y398A (2 ng RNA) rescues lamellipodia inhibited by nocodazole (15 μg/ml). (S,T) XLfc C55R (250 pg DNA) inhibits lamellipodial protrusions and cell-cell contact.

Fig. 3. Velocity of microtubule growth does not change between stages 10 and 10.5. (A) eGFP-CLIP-170 marks growing ends of microtubules in explants. (B) Velocities of microtubule growth in explants, either stage 10 or 10.5. Each point represents an individual microtubule tracked for at least 20 seconds.

unrelated to nocodazole, produced the same effects (data not shown).

The loss of cell-cell contacts may be a consequence of the loss of actin-based protrusions. Latrunculin B, a small molecule that induces actin depolymerization, caused rapid and severe loss of active protrusions and cell-cell contact, inhibiting convergent extension movements (Fig. 4). This, coupled with the significant delay in the loss of cell-cell contact relative to the inhibition of active protrusions following exposure to nocodazole, suggests that loss of cell-cell contact may be a secondary effect of microtubule depolymerization.
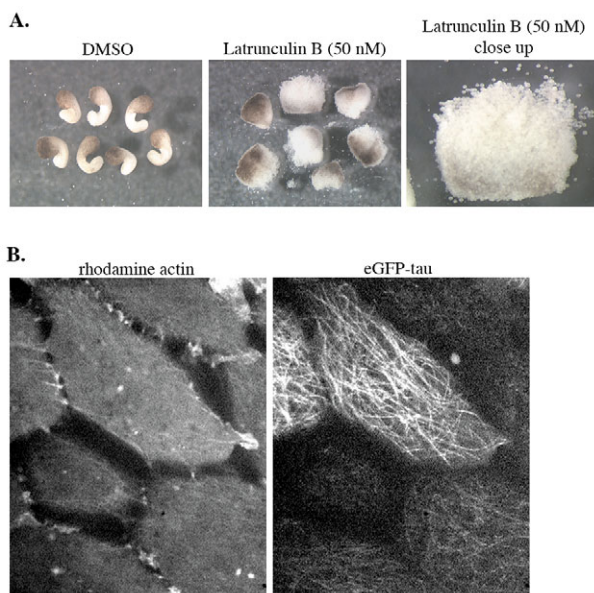
Microtubule structure, dynamics are equally sensitive to nocodazole after stage 10.5

Why are explants stage 10.5 or older insensitive to nocodazole? We tested whether there might be a large-scale change in the structure, stability, or dynamics of the microtubule cytoskeleton. For example, drug-resistant microtubules are seen in neurons and other cell types (Bulinski and Gundersen, 1991). As shown in Fig. 2H, microtubules in explants stage 10.5-11 were depolymerized by nocodazole, as indicated by diffuse eGFP-tau fluorescence. Notably, lamellipodia were not inhibited by nocodazole or colcemid after stage 10.5, whereas they were before stage 10.5 (compare Fig. 2G with Fig. 2C,E).

Microtubule dynamics are not obviously different after stage 10.5. Velocity measurements of microtubule plus-end growth (using eGFP-CLIP-170, 300 pg RNA) revealed that dynamic growth was not significantly different before and after stage 10.5. In Fig. 3B, each point represents the velocity of growth of a single microtubule, tracked for at least 20 seconds. Blue points are microtubules from stage 10 explants (37 microtubules from eight cells in two explants), while red points are microtubules from stage 10.5 explants (34 microtubules from seven cells in two explants). At stage 10, the average velocity of microtubule growth was 0.514 ± 0.042 μm/sec, while at stage 10.5, the average velocity was 0.486 ± 0.056 μm/sec; there was no significant change in velocity of growth. These data suggest that significant changes in the microtubule cytoskeleton or dynamics are not responsible for the change in the sensitivity of convergent extension to microtubule depolymerization. It should be noted, however, that these experiments have only monitored the velocity of microtubule growth, not disassembly, as eGFP-CLIP-170 marks only growing ends of microtubules. As a result, it is possible that there is a change in the velocity of microtubule disassembly, the proportion of microtubules undergoing shrinkage, or the fraction of stable microtubules. However, the similar growth characteristics of microtubules and continued sensitivity to nocodazole suggest that their intrinsic properties change little, if at all, between stages 10 and 10.5.

Microtubule mass is a crucial factor in convergent extension

It has been reported that the microtubule-stabilizing drug taxol has no effect on convergent extension movements (Lane and Keller, 1997). Although taxol stabilizes, rather than depolymerizes, microtubules, it also interferes with dynamic functions of microtubules. We have confirmed the insensitivity

Fig. 4. Latrunculin B inhibits convergent extension by inducing cell dissociation and preventing the explant from rounding up. (A) Morphology of explants treated with latrunculin B. Note the rectangular shape of explants, which have not healed nor undergone convergent extension, as well as the dissociation of the cells in the closeup picture. (B) Confocal microscopy of an explant treated with latrunculin B (50 nM). Note the loss of lamellipodial protrusions and cell-cell contact (rhodamine actin), although the microtubule cytoskeleton remains intact (eGFP-tau). This effect was found for latrunculin B concentrations starting at 25 nM. Lower concentrations (5 or 15 nM) resulted in a lack of actin depolymerization (as demonstrated by confocal microscopy), and, as a result, the explants healed and underwent convergent extension movements normally. Data are from one representative experiment of four trials, analyzing six to seven explants per sample in each trial.

to taxol, using continuous treatment of explants with taxol (20 μg/ml) from stage 10 to 19 (Fig. 5A,B). Confocal microscopy revealed that unlike nocodazole, taxol had no effect on active protrusions or cell-cell contacts (Fig. 2I). Taxol-stabilized microtubules bound eGFP-CLIP-170 uniformly, not just at their plus-ends, an indication that the microtubules are static (Fig. 2J).

Taxol treatment, while abolishing the dynamic properties of microtubules, left them structurally intact, allowing continued interaction with microtubule-associated proteins and vesicular trafficking via motor proteins. To distinguish the role of polymer mass independent of microtubule structure, we utilized another pharmacological inhibitor of microtubule dynamics, vinblastine. In mammalian cells, high concentrations of vinblastine completely convert microtubules into paracrystalline arrays of tubulin protofilaments, which have none of the biological features of microtubules that rely on their dynamics. As shown in Fig. 5C, vinblastine (2 μM) induced paracrystalline arrays of tubulin in *Xenopus* explants; however, continuous exposure of explants to vinblastine from stage 10 to 19 did not significantly inhibit convergent extension (Fig. 5D,E).

Although taxol and vinblastine inhibit microtubule dynamics, the stabilized microtubules or tubulin protofilaments are in a conformation to which microtubule-associated proteins can still bind; proteins that might bind to microtubules under normal conditions should still bind in the presence of either taxol or vinblastine. These data suggest that although there is a microtubule requirement at stage 10 for convergent extension, the requirement does not include the structure and dynamics of the microtubule array. Instead, the crucial microtubule requirement during convergent extension is protofilament mass.

Fig. 5. Taxol and vinblastine do not inhibit convergent extension. (A) Morphology of explants treated with taxol. (B) Length/width ratios of explants in (A). (C) Tubulin staining (DM1α) in vinblastine-treated explants. Note crystalline arrays of tubulin in vinblastine-treated cells. (D) Morphology of explants treated with vinblastine. (E) Length/width ratios of explants in (D). Data are from one representative experiment of three trials (for each taxol and vinblastine), analyzing six to seven explants per sample per trial.

The microtubule mass requirement can be rescued by dominant negative Rho and Rho-kinase inhibitor

The link between microtubules and actin has not been shown to be a direct physical one, which suggests a role of microtubules in regulating signaling or other activities. Small GTPases of the Rho family have long been demonstrated to regulate cell morphology and the actin cytoskeleton (Hall and Nobes, 2000). These small GTPases, including Rac, Rho and Cdc42, cycle between an active, GTP-bound state, and an inactive, GDP-bound state. The nucleotide state of the GTPase is regulated intrinsically by the nucleotide hydrolysis activity of the GTPase, and extrinsically by factors such as guanine-nucleotide exchange factors (GEFs) and GTPase-activating proteins (GAPs). There is evidence that microtubule depolymerization can lead to the activation of certain Rho-family GTPases, which then induce changes in cell morphology (Etienne-Manneville and Hall, 2002). In HeLa cells, microtubule depolymerization induces cell retraction and formation of stress fibers, a phenotype characteristic of Rho activation (Krendel et al., 2002). Based
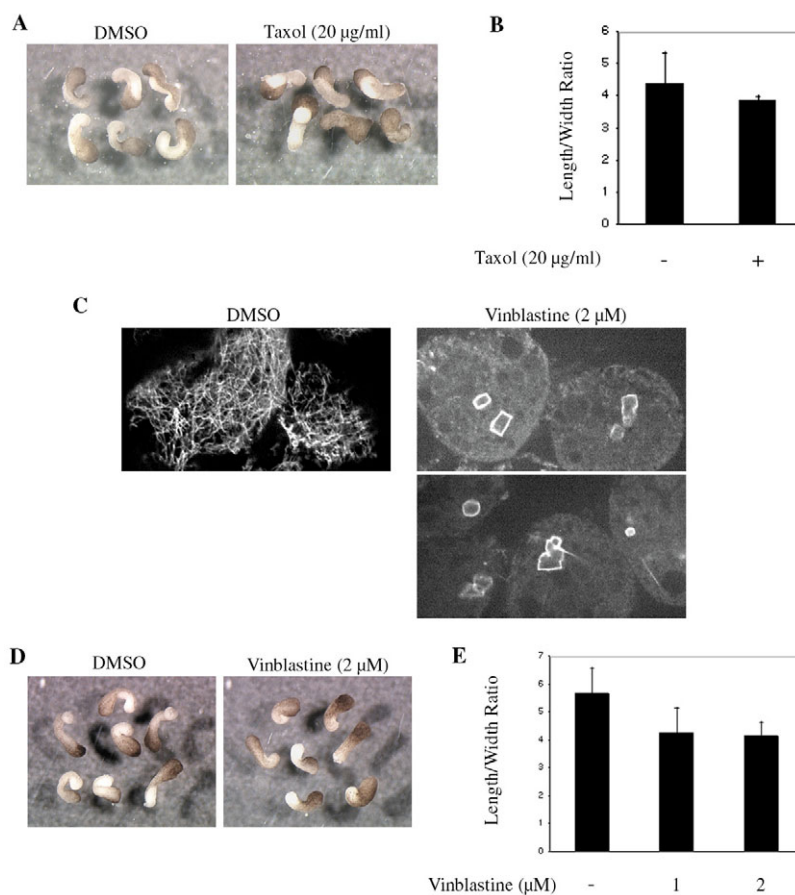
on this, we tested the involvement of Rho in convergent extension.

We injected RNA encoding a dominant negative (dn) Rho mutant (N19) into the prospective DMZ of the 4-cell embryo. We found that dn Rho (200 or 400 pg RNA) partially rescued the effects of nocodazole on convergent extension (Fig. 6A,B). When treated with nocodazole (15 μg/ml), the extension of explants expressing dn Rho was statistically greater than of those not expressing dn Rho (*P*<0.05). When dn Rho was co-injected with rhodamine-actin (15 ng) and eGFP-tau (100 pg RNA), confocal microscopy revealed that although microtubules in the explant remained depolymerized, dn Rho rescued the inhibition of lamellipodia caused by nocodazole (Fig. 2K,L).

As dn Rho rescued the inhibition of convergent extension by nocodazole, we tested the involvement of a downstream effector of Rho, Rho kinase, via the small molecule inhibitor Y-27632. Inhibition of Rho kinase (10 μM Y-27632) partially rescued the inhibition of convergent extension by nocodazole (Fig. 6C,D). The extent of elongation in explants treated with both nocodazole and Y-27632 was significantly greater than the elongation of explants treated only with nocodazole (*P*<0.01).

Y-27632 also rescued the inhibition of lamellipodia by nocodazole, without affecting nocodazole-mediated microtubule depolymerization (Fig. 2M,N).

These data suggest that activation of the small GTPase Rho, and subsequently its downstream effector Rho kinase, could be at least partially responsible for mediating the effects of microtubule depolymerization.

The microtubule depolymerization effects can be overcome by V12 Rac, but not V12 Cdc42

Because actin assembly and protrusive activity can be mediated by Rac and Cdc42, we asked whether the nocodazole-mediated inhibition of convergent extension could be overcome by activated forms of Rac (V12) or Cdc42 (V12). In mammalian cell culture, activated Rac induces the formation of lamellipodia, while activated Cdc42 induces the formation of filopodia (Nobes and Hall, 1995); these effects are recapitulated in *Xenopus* cells (Hens et al., 2002; Kwan and Kirschner, 2003). Therefore, active protrusions induced by these proteins might bypass the effects of microtubule depolymerization, thereby rescuing convergent extension movements.

V12 Rac (25 pg DNA) partially overcame the inhibition of convergent extension by nocodazole (Fig. 7A,B). The extent of elongation in explants expressing V12 Rac and treated with nocodazole (15 µg/ml) was significantly greater than the elongation of explants treated with only nocodazole ($P<0.05$). Confocal microscopy revealed that active protrusions were restored, even though microtubules remained depolymerized (Fig. 2O,P). It should be noted that higher amounts of V12 Rac (50-200 pg DNA) did not rescue convergent extension. Under these conditions, cells are unpolarized, displaying protrusive activity around the entire perimeter of the cells (data not shown). Such dysregulation of active protrusions has been shown to be sufficient to inhibit convergent extension (Wallingford et al., 2000). When V12 Cdc42 was tested for its ability to rescue convergent extension blocked by nocodazole, it was ineffective (Fig. 7C,D). This was true over the entire range of DNA concentrations tested (25-100 pg DNA).

These data suggest that induction of lamellipodia by V12 Rac, and not induction of filopodia by V12 Cdc42, is sufficient to overcome nocodazole-mediated inhibition of convergent extension.

Cloning and alignment of XLfc

We have shown that a sufficient mass of oligomerized or polymerized tubulin is crucial for convergent extension, and that dn Rho, Rho kinase inhibition, and activated Rac can partially overcome the inhibition of convergent extension by nocodazole. This is reminiscent of a phenomenon reported in HeLa cells, where microtubule depolymerization induces cell retraction and formation of stress fibers downstream of Rho (Krendel et al., 2002). A microtubule-binding Rho-GEF, GEF-H1, was identified, which is inactivated by binding to microtubules. Microtubule depolymerization liberates GEF-H1, which activates Rho; Rho then induces cell retraction and stress fiber formation.

A small fragment of the *Xenopus* homolog of GEF-H1 had already been cloned (Morgan et al., 1999). *Xenopus* Lfc (XLfc, after the mouse homolog of GEF-H1, Lfc) was reported to be a zygotic transcript, with expression beginning at stage 9.5 (late blastula). In-situ analysis demonstrated that XLfc is expressed in the ectoderm and mesoderm, with expression restricted to the neural ectoderm during neurula stages (Morgan et al., 1999). As XLfc is expressed at the right time and place to be involved in convergent

Fig. 6. Dominant-negative Rho and Rho-kinase inhibitor partially rescue the effects of nocodazole on convergent extension. (A) Morphology of explants treated with nocodazole and expressing dn Rho. (B) Length/width ratios of explants in (A). *$P<0.05$, as calculated by Tukey's method. (C) Morphology of explants treated with nocodazole and Rho-kinase inhibitor Y-27632. (D) Length/width ratios of explants in (C). *$P<0.01$, as calculated by Tukey's method. Data are from one representative experiment of five trials (dn Rho), and three trials (Y-27632), analyzing six to seven explants per sample per trial.
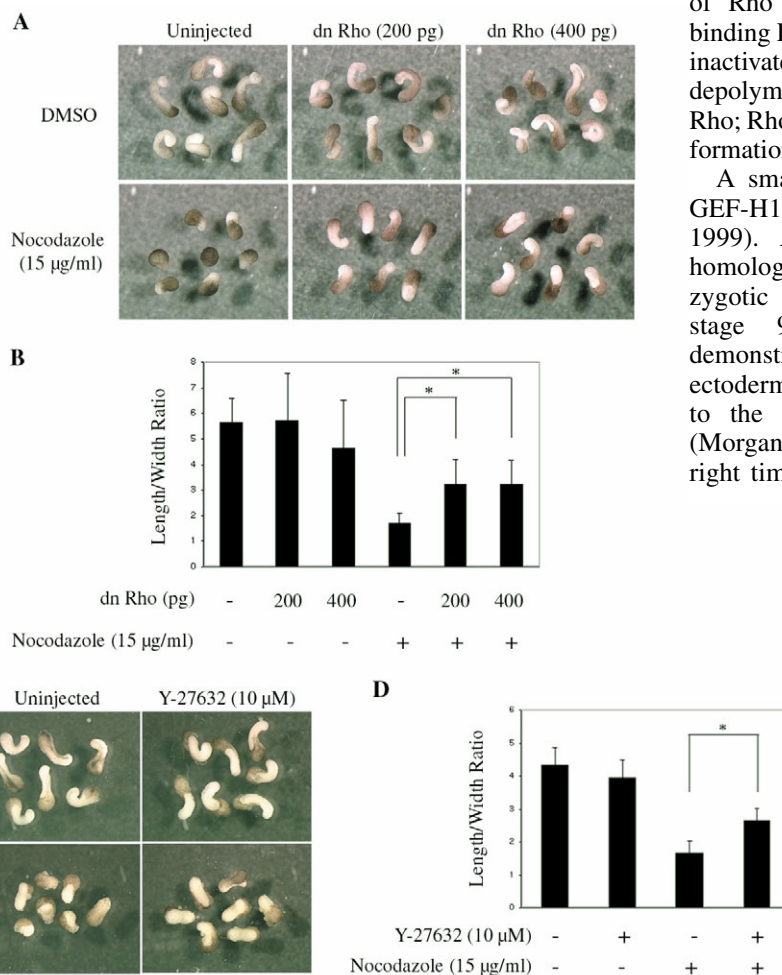
extension, we cloned the full-length gene to see if its activity is responsible for the effects induced by microtubule depolymerization.

Full-length XLfc is 981 amino acids (Fig. 8A), with a predicted molecular weight of 131 kD. Like its mouse and human homologs, XLfc contains a C1/zinc-binding region near the N-terminus, which has been demonstrated to be required for microtubule binding (Krendel et al., 2002), as well as a Dbl-homology (DH) domain, responsible for nucleotide exchange activity, a pleckstrin-homology (PH) domain, and a coiled-coil (CC) region.

As localization of GEF-H1 and Lfc to microtubules is crucial for regulation of nucleotide exchange activity, the localization of XLfc was tested. NIH3T3 cells were transfected with eGFP-XLfc, fixed, and stained for eGFP and tubulin. In transfected cells, eGFP-XLfc colocalizes with microtubules (Fig. 8B).
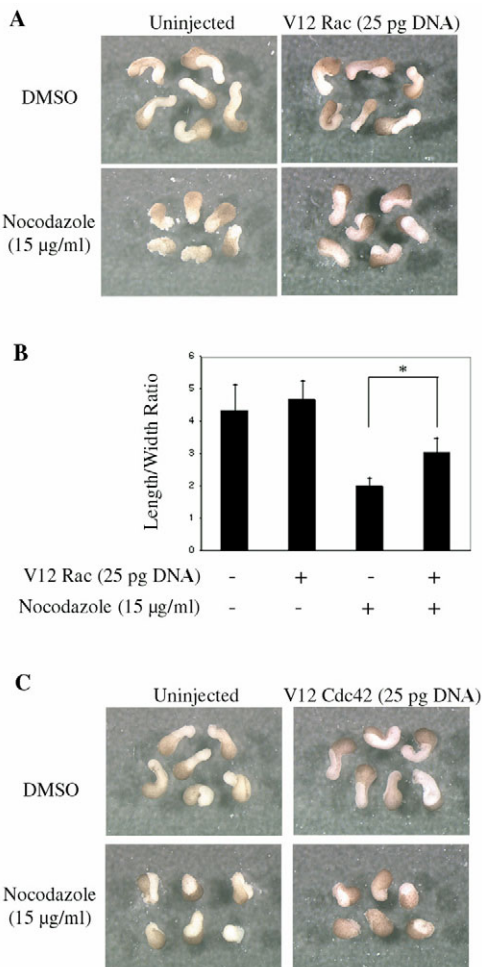

Fig. 7. Activated Rac, but not activated Cdc42, partially overcomes the effects of nocodazole on convergent extension. (A) Morphology of explants treated with nocodazole and expressing V12 Rac. (B) Length/width ratios of explants in (A). *$P<0.05$, as calculated by Tukey's method. (C) Morphology of explants treated with nocodazole and expressing V12 Cdc42. (D) Length/width ratios of explants in (C). Data are from one representative experiment of three trials (V12 Rac), and two trials (V12 Cdc42), analyzing six to seven explants per sample per trial.

The effects of microtubule depolymerization are rescued by dominant negative XLfc and recapitulated by activated XLfc

To determine whether XLfc nucleotide exchange activity is required for the inhibition of convergent extension by microtubule depolymerization, we generated a dominant negative construct with a point mutant in the conserved QRITKY motif in the Dbl homology domain, the domain responsible for nucleotide exchange activity. Tyr 398 was
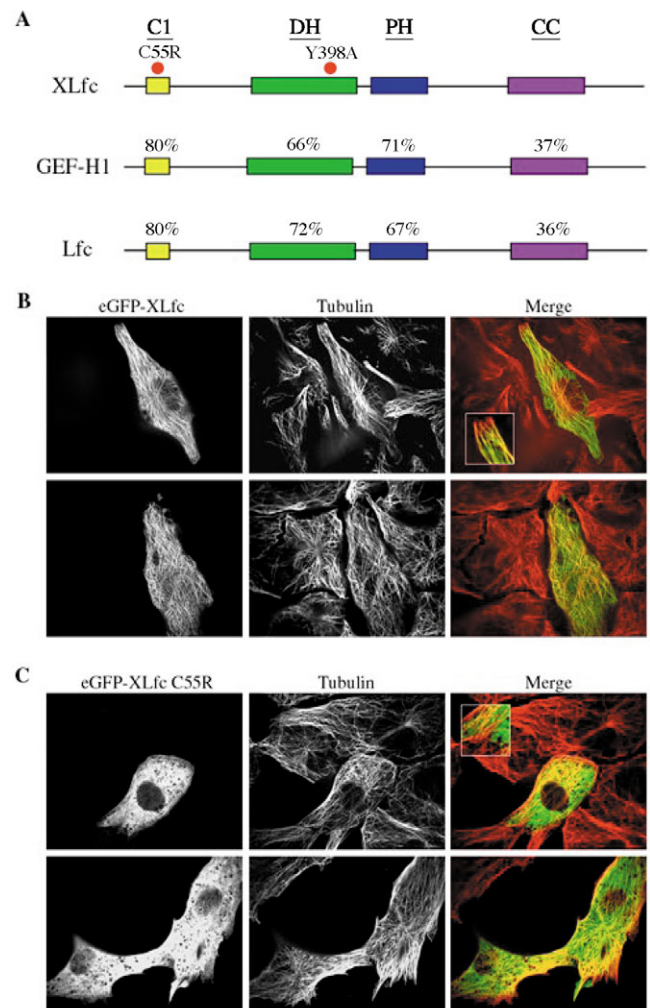

Fig. 8. XLfc alignment and localization. (A) Alignment of XLfc with homologs GEF-H1 (human) and Lfc (mouse). Yellow marks C1/zinc-binding domain, green marks Dbl homology (DH) domain, blue marks pleckstrin homology (PH) domain, and purple marks coiled-coil (CC) region. XLfc C55, marked with a red dot, is mutated to arginine for the non-microtubule binding constitutively active mutant. XLfc Y398, also marked with a red dot, is mutated to alanine for the catalytically dead dominant negative mutant. Numbers indicate percent identity between XLfc and its homologs. (B) eGFP-XLfc localizes to microtubules in NIH3T3 cells. Cells were transfected, fixed and stained for eGFP and tubulin. Inset: magnified view of colocalization of eGFP-XLfc (green) with microtubules (red). (C) eGFP-XLfc C55R does not localize to microtubules in NIH3T3 cells. Inset: magnified view of eGFP-XLfc C55R (green) and microtubules (red). Note cytoplasmic, non-filamentous localization of eGFP-XLfc C55R.

Development

converted to Ala; the analogous mutation in GEF-H1 abolishes nucleotide exchange activity in vitro (Krendel et al., 2002; Sterpetti et al., 1999). XLfc Y398A (1 or 2 ng RNA) partially rescued nocodazole-mediated inhibition of convergent extension (Fig. 9A,B). The elongation of explants expressing XLfc Y398A and treated with nocodazole was significantly greater than elongation in explants treated only with nocodazole ($P<0.05$). Confocal microscopy revealed that cell-cell contact and active protrusions were restored (Fig. 2Q,R). These data suggest that XLfc nucleotide exchange activity is required for nocodazole to inhibit convergent extension. It should be noted that wild-type XLfc, by contrast, has a weakly inhibitory effect on convergent extension on its own, and was not tested for its ability to rescue the effects of microtubule depolymerization on convergent extension (data not shown).

According to the current model for regulation of XLfc family members, sequestration by microtubules inhibits GEF activity; conversely, release from microtubules or the inability to bind microtubules results in high GEF activity (Krendel et

al., 2002). In this case, a form of XLfc unable to bind microtubules should recapitulate the effects of nocodazole on convergent extension. Previously, a mutation in the GEF-H1 C1/zinc-binding region (C53R) was found to abolish microtubule localization in HeLa cells, and exhibit high GEF activity (Krendel et al., 2002). We made the analogous point mutant (C55R) and tested its ability to localize to microtubules in NIH3T3 cells. Unlike wild-type XLfc, which localizes to microtubules, eGFP-XLfc C55R displayed a diffuse cytoplasmic localization (Fig. 8C), consistent with an inability to bind microtubules. XLfc C55R (175 and 250 pg DNA) inhibited convergent extension in the absence of nocodazole (Fig. 9C,D). By contrast, wild-type XLfc had only a weak inhibitory effect at similar concentrations (data not shown). Confocal microscopy revealed inhibition of lamellipodia and loss of cell-cell contact; however, the microtubule cytoskeleton was completely intact (Fig. 2S,T). Whole embryos expressing XLfc C55R displayed defects in convergent extension (Fig. 9E). This suggests that activation of XLfc is sufficient to inhibit lamellipodial protrusions, and, as a result, convergent extension. In effect, we have uncoupled the effects of microtubule depolymerization from the effects on lamellipodial protrusions.

Morpholino knockdown of XLfc diminishes the effects of microtubule depolymerization on convergent extension

While the dominant negative and constitutively active XLfc results support the argument that overexpression of altered forms of XLfc can affect convergent extension, we wanted to determine whether XLfc is required for the effects of nocodazole on convergent extension. Our hypothesis suggests that if XLfc is a major effector of microtubule depolymerization, knockdown of XLfc will block the ability of nocodazole to inhibit convergent extension. To test the requirement for XLfc in mediating the effects of nocodazole, we designed a translation-blocking morpholino against XLfc (MoXLfc); embryos were injected in both cells of the 2-cell stage with morpholino oligonucleotides. Knockdown of XLfc diminished the inhibition of convergent extension by nocodazole, in a dose-dependent manner (Fig. 10A,B). A control morpholino (MoCon) with the same nucleotide composition as MoXLfc had no effect. Interestingly, knockdown of XLfc had no effect on
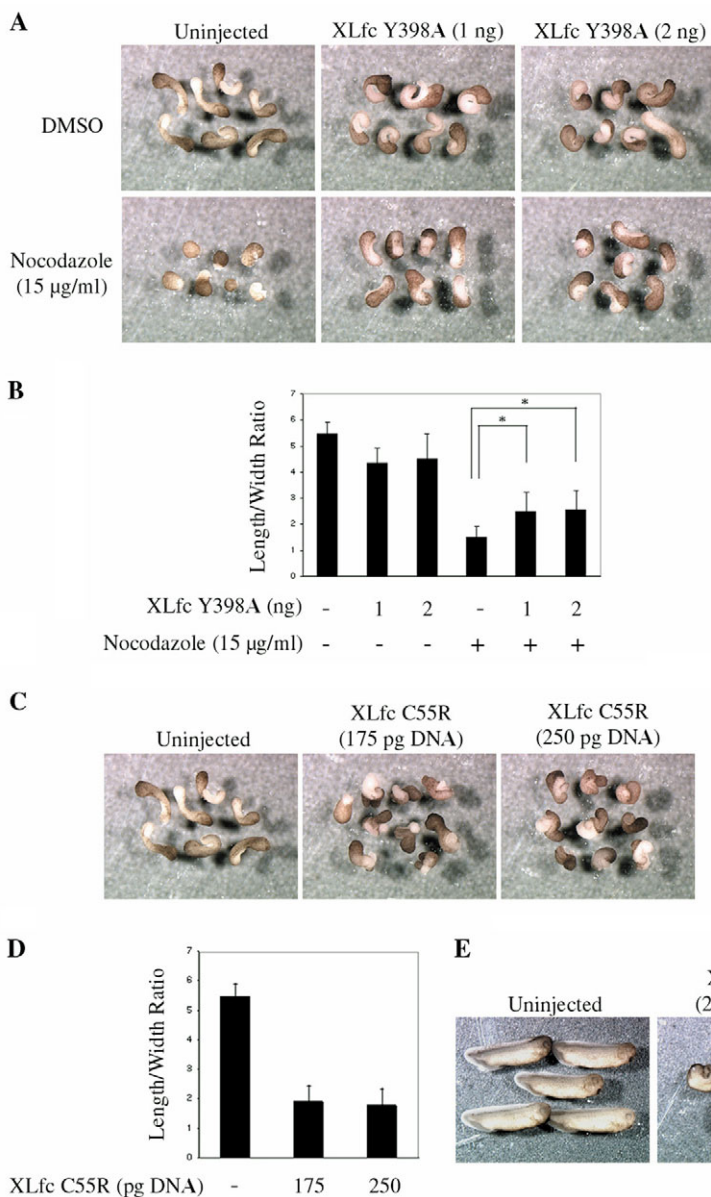

Fig. 9. XLfc nucleotide exchange activity is required for inhibition of convergent extension by nocodazole; constitutively active XLfc is sufficient to inhibit convergent extension. (A) Morphology of explants treated with nocodazole and expressing XLfc Y398A. (B) Length/width ratios of explants in (A). *$P<0.05$, as calculated by Tukey's method. (C) Morphology of explants expressing XLfc C55R. (D) Length/width ratios of explants in (C). (E) Whole embryos expressing XLfc C55R display convergent extension defects. Data are from one representative experiment of three trials for both XLfc Y398A and XLfc C55R, analyzing six to nine explants per sample per trial.

Development

convergent extension without the addition of nocodazole (see Discussion).

To confirm the specificity of the morpholino effects, we designed a version of full-length XLfc not recognized by the morpholino; the amino acid sequence is conserved while the nucleotide sequence is altered. This version of XLfc is referred to as wobbled-XLfc (wXLfc). For these experiments, embryos were first injected at the 2-cell stage with morpholinos. At the 4-cell stage, embryos were injected in the DMZ with wXLfc RNA. At these doses, expression of wXLfc alone had only modest effects on convergent extension (Fig. 10C, compare panels I and III); because wXLfc has an intact microtubule-binding site, it is presumably buffered by microtubules.

Expression of wXLfc restored, in a dose-dependent manner, the ability of nocodazole to inhibit convergent extension (Fig. 10C, panel II). These data suggest that XLfc is a major endogenous effector of microtubule depolymerization during convergent extension.

Discussion

During early development of *Xenopus*, convergent extension serves to narrow and lengthen the embryo along the anterior-posterior dimension. While many developmental genes regulating convergent extension have been identified, little is understood about the cell biological basis of these movements.
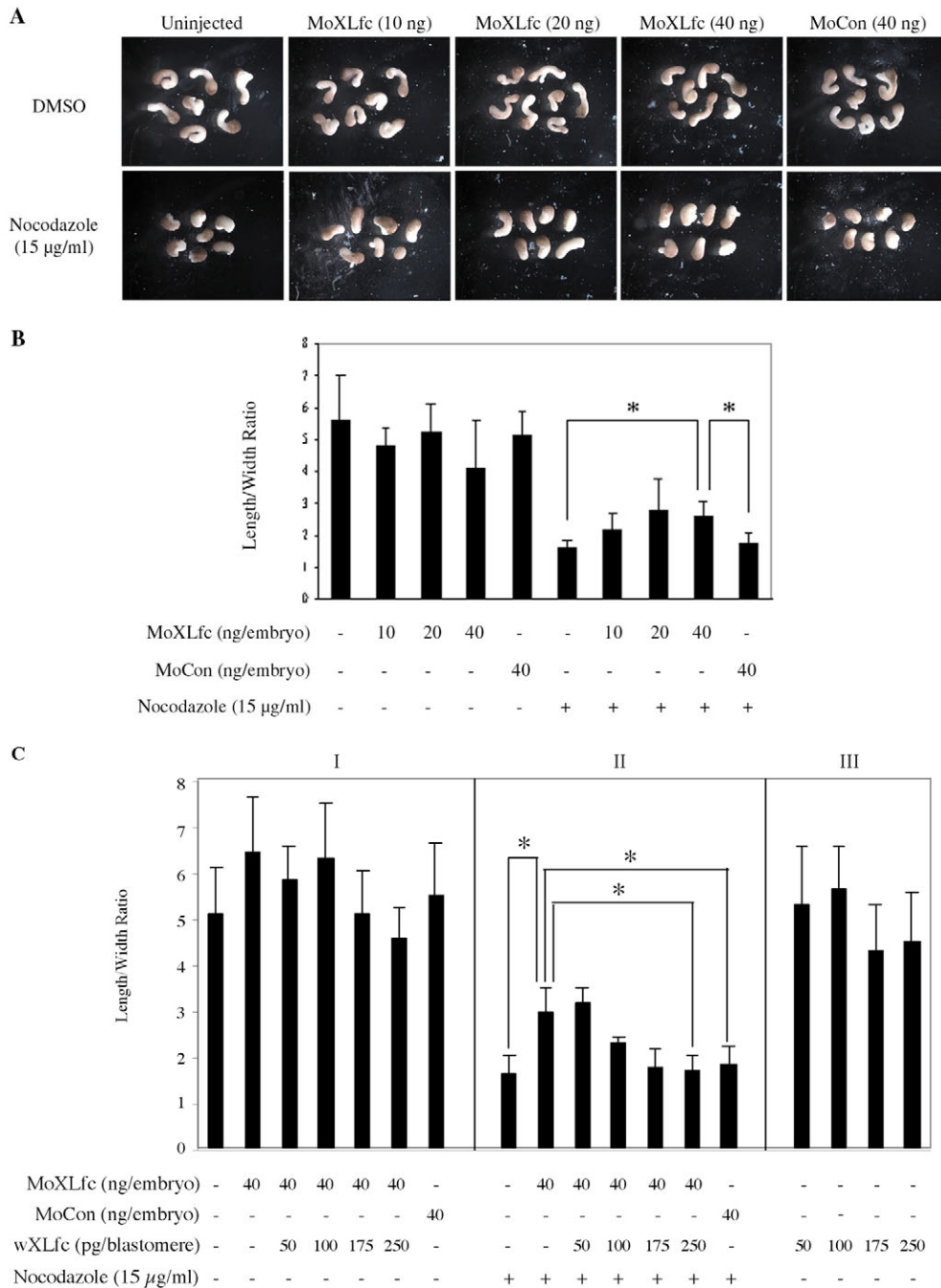

Fig. 10. Morpholino knockdown of XLfc diminishes the ability of nocodazole to inhibit convergent extension. (A) Morphology of explants treated with nocodazole and injected with morpholino against XLfc (MoXLfc) or control morpholino (MoCon). (B) Length/width ratios of explants in (A). *$P<0.05$, as calculated by Tukey's method. (C) Length/width ratios of explants treated with nocodazole and injected with morpholinos and wobbled XLfc (wXLfc) rescue RNA. *$P<0.01$, as calculated by Tukey's method. Data are from one representative experiment of four trials (morpholino knockdown), and two trials (wXLfc rescue), analyzing six to seven explants per sample per trial.

Microtubules were previously shown to be required for convergent extension (Lane and Keller, 1997), although only for a specific time period. Microtubules are known to be involved in cell polarity, but in some cases (e.g. leukocyte chemotaxis), the actin cytoskeleton can support cell polarity without microtubules. In convergent extension, mediolateral cell polarity involves actin-based lamellipodial protrusions. Therefore, this system presents a novel developmental context in which to explore microtubule-actin crosstalk.

At the cellular level, there were two effects of microtubule depolymerization on convergent extension. Within 30 minutes of nocodazole addition, active protrusions ceased; lamellipodia were inhibited. By 1 to 3 hours of nocodazole exposure, cell-cell contacts were inhibited. We hypothesize that loss of cell-cell contact is an indirect effect of having lost active protrusions, because of the time difference in effects, and also because targeting actin filaments directly (via latrunculin B) inhibits active protrusions and rapidly induces dissociation (Fig. 4). We therefore sought a connection between microtubule depolymerization and lamellipodial retraction that would occur within 30 minutes.

We have confirmed that there is an abrupt switch at stage 10.5, after which convergent extension is insensitive to microtubule depolymerization (Lane and Keller, 1997). This switch does not seem to correspond to changes in the structure or dynamics of the microtubule cytoskeleton (Fig. 2G,H and Fig. 3). It seemed unusual that convergent extension is not affected by either taxol or vinblastine, both of which impair filament organization and dynamics in mechanistically distinct ways from each other and from nocodazole. Taxol stabilizes microtubule polymers but completely blocks dynamics. Vinblastine completely dissolves microtubules, dissembling them into short protofilaments that aggregate into large paracrystals. Although normal microtubule functions are inhibited, both of these represent stabilized forms of tubulin polymer still capable of binding microtubule-associated proteins. The most likely explanation for the sensitivity of convergent extension to nocodazole and insensitivity to vinblastine and taxol is that it is not microtubule dynamics that are important, but simply the mass of assembled protofilaments.

Because of the effects of nocodazole on lamellipodial protrusions, we tested the role of Rho-family GTPases downstream of microtubule depolymerization. Inhibition of convergent extension by nocodazole could be partially rescued by dn Rho (N19), Rho-kinase inhibitor (Y-27632), or V12 Rac (Fig. 6, Fig. 7A,B). Confocal microscopy revealed that each of these factors restored lamellipodia, suggesting that microtubule depolymerization inhibits convergent extension via alterations of the actin cytoskeleton (Fig. 2K-P). Similarly, it has been demonstrated that alterations of active protrusions are sufficient to inhibit convergent extension (Wallingford et al., 2000). It is worth mentioning that some of the factors tested here, such as Rho and Rho kinase, can, at high levels, inhibit convergent extension (Marlow et al., 2002; Tahinci and Symes, 2003). In the experiments reported here, we have used levels of dn Rho and Rho-kinase inhibitor 2- to 4-fold lower than the levels that inhibit convergent extension. There exists a continuum of effects that goes from no protrusive activity (convergent extension is blocked), to sufficient protrusive activity to maintain polarity (favoring convergent extension),

to exuberant protrusive activity (polarity is lost and convergent extension is again blocked). For example, with V12 Rac, 25 pg DNA is sufficient to overcome the inhibition of convergent extension by nocodazole, but higher amounts (50-200 pg DNA) induce lamellipodia indiscriminately, in an unpolarized manner, and block convergent extension (data not shown). This suggests that whatever signals lead to cell polarization, directed motility can be blocked by inhibition of protrusive activity and also by excessive protrusive activity that occurs around the entire cell. This underscores the dynamic nature of the process; although many cell biological regulators are required for convergent extension, their levels and activity must be tightly regulated. It has been previously noted that the expression level of many regulators is crucial for convergent extension (Djiane et al., 2000; Wallingford et al., 2002).

Microtubule depolymerization in HeLa cells induces cell retraction and stress fiber formation, as a result of Rho activation. These effects can be accounted for by activation of the microtubule-binding Rho-GEF, GEF-H1 (Krendel et al., 2002). We have cloned the full-length *Xenopus* homolog of GEF-H1, XLfc (Fig. 8A). Previously, a partial clone of XLfc was isolated (Morgan et al., 1999); in-situ analysis revealed that XLfc is expressed at the right time and place to be involved in convergent extension. Dominant negative XLfc (Y398A), which lacks nucleotide exchange activity, partially rescued the effects of nocodazole on convergent extension (Fig. 2Q,R, Fig. 9A,B), suggesting that nucleotide exchange activity of XLfc is required for microtubule depolymerization to inhibit convergent extension. Conversely, constitutively active XLfc (C55R), which does not localize to microtubules, is sufficient to inhibit convergent extension (Fig. 9C-E), recapitulating the effects of microtubule depolymerization at the cellular level: inhibition of lamellipodia and loss of cell-cell contact (Fig. 2S,T).

Although dominant negative and constitutively active forms of XLfc affected convergent extension in the manner expected, this did not test directly the role of XLfc in convergent extension. Therefore, we designed a translation-blocking morpholino to knockdown endogenous XLfc. We reasoned that if nocodazole acts via XLfc, knockdown of XLfc would block the ability of nocodazole to inhibit convergent extension. XLfc morpholino diminished, in a dose-dependent manner, the ability of nocodazole to inhibit convergent extension (Fig. 10A,B). Expression of a wobbled XLfc construct not recognized by the morpholino restored the ability of nocodazole to inhibit convergent extension (Fig. 10C). Interestingly, knockdown of XLfc had no discernible effect on convergent extension in the absence of nocodazole, suggesting that under normal circumstances, endogenous polarization cues are strong enough to overcome the lack of XLfc, or that reduced levels of XLfc are still sufficient to carry out normal function. Alternately, as knockdown of XLfc gives only a partial block of the nocodazole effect, there may be other XLfc-like genes not recognized by the morpholino that can partially compensate in the absence of XLfc. In any case, the loss-of-function experiment suggests that XLfc is a major endogenous effector of microtubule depolymerization during convergent extension.

As XLfc activity is regulated by microtubules, at least before stage 10.5, we asked why such an unusual mechanism of regulation, among the many transcriptional, translational and
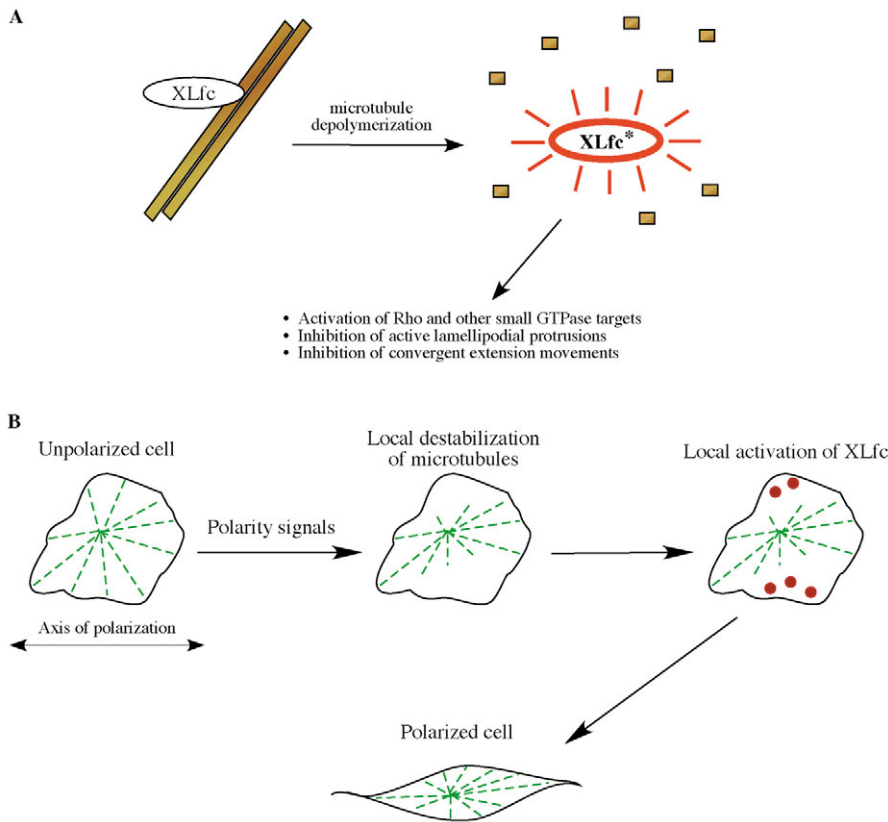
A

- Activation of Rho and other small GTPase targets
- Inhibition of active lamellipodial protrusions
- Inhibition of convergent extension movements

B

Fig. 11. Current models of XLfc action. (A) XLfc regulation by microtubules: when bound to microtubules, XLfc is inactive. Upon microtubule depolymerization, XLfc is released and becomes active for nucleotide exchange activity. Active XLfc activates Rho-family GTPases, which inhibit lamellipodial protrusions and cell-cell contact. (B) Working model for how XLfc contributes to establishment of cell polarity. Polarity cues alter local microtubule stability; local microtubule depolymerization leads to local activation of XLfc. XLfc induces local inhibition of lamellipodial protrusions.

post-translational means available. The unique feature of microtubules is that their distribution (and hence, mass) is non-uniform, dynamic and reflective of overall cell polarity. Summarizing our current model of XLfc regulation (Fig. 11A), XLfc binds microtubules and is inactive. Upon microtubule depolymerization, XLfc is released and becomes active for nucleotide exchange activity, thereby activating certain Rho-family GTPases. Activation of Rho-family GTPases leads to inhibition of lamellipodia and loss of cell-cell contact.

These data suggest that XLfc could be a crucial and novel regulator of cell morphology during convergent extension and perhaps other processes. Because deregulation of XLfc is sufficient to uncouple the effects of microtubule depolymerization from changes in actin-based cell morphology, and because the developmental switch at stage 10.5 effectively does the same, regulation of XLfc protein or activity may account for the change in sensitivity of convergent extension to nocodazole, and may reflect a regulatory shift in controlling cell polarity at that stage.

While it is possible that global regulation of XLfc by microtubule polymer creates permissive conditions for lamellipodial activity and convergent extension, microtubule binding creates the opportunity for XLfc to act locally within cells; a speculative model is schematized (Fig. 11B). While we might expect the steady state concentration of unbound XLfc to be uniform in the cell, this might not be true in transient states. Episodes of microtubule turnover could induce local Rho activation and inhibition of lamellipodia. Such local effects could help break the symmetry of lamellipodial extension around the entire periphery of the cell. This proposed model is consistent with the original work describing the

establishment of polarity during convergent extension (Shih and Keller, 1992). The crucial step in establishment of polarity is not induction of polarized mediolateral protrusions, but loss or repression of anterior-posterior protrusions. Identification of the signals inducing polarization during convergent extension will greatly aid the dissection of these models.

It is important to point out that dn Rho only partially rescued nocodazole-mediated inhibition of convergent extension, suggesting that Rho may not be the relevant or only target of XLfc. Two different forms of activated Rho (V14 and L30) do not fully recapitulate the effects of microtubule depolymerization on convergent extension (data not shown). V14 Rho can indeed inhibit convergent extension, but lamellipodia are not lost (data not shown). This result was also obtained in a study of GTPase overexpression during convergent extension (Tahinci and Symes, 2003). These observations reinforce the importance of combining whole explant analysis with cellular-level analysis. While inhibition of lamellipodial protrusions is sufficient to inhibit convergent extension, other mechanisms (e.g. subtle changes in cell morphology and dynamics of active protrusions) are likely to be important and merit further analysis. One hundred small GTPases have been tested in a simple morphological assay; HeLa cells were transfected and observed for changes in cell shape, polarity, and spreading (Heo and Meyer, 2003). This work suggests that considering only Rac, Rho and Cdc42 is inadequate when evaluating cell morphology. Unfortunately, these reagents are not readily available; therefore, it was not possible for us to test involvement of other Rho-family GTPases in convergent extension. It is likely that XLfc activates one or more small GTPases in addition to Rho; the

activity of these targets alone or in combination with Rho would be responsible for mediating the effects of XLfc, which are clearly revealed only under conditions of microtubule depolymerization.

Supplementary material

Supplementary material for this article is available at
http://dev.biologists.org/cgi/content/full/132/20/4599/DC1

References

Bulinski, J. C. and Gundersen, G. G. (1991). Stabilization of post-translational modification of microtubules during cellular morphogenesis. *Bioessays* **13**, 285-293.

Djiane, A., Riou, J., Umbhauer, M., Boucaut, J. and Shi, D. (2000). Role of frizzled 7 in the regulation of convergent extension movements during gastrulation in *Xenopus laevis*. *Development* **127**, 3091-3100.

Etienne-Manneville, S. and Hall, A. (2002). Rho GTPases in cell biology. *Nature* **420**, 629-635.

Gerhart, J. and Keller, R. (1986). Region-specific cell activities in amphibian gastrulation. *Annu. Rev. Cell Biol.* **2**, 201-229.

Hall, A. and Nobes, C. D. (2000). Rho GTPases: molecular switches that control the organization and dynamics of the actin cytoskeleton. *Philos. Trans. R. Soc. London Ser. B* **355**, 965-970.

Hens, M. D., Nikolic, I. and Woolcock, C. M. (2002). Regulation of *Xenopus* embryonic cell adhesion by the small GTPase, rac. *Biochem. Biophys. Res. Commun.* **298**, 364-370.

Heo, W. D. and Meyer, T. (2003). Switch-of-function mutants based on morphology classification of Ras superfamily small GTPases. *Cell* **113**, 315-328.

Keller, R., Davidson, L., Edlund, A., Elul, T., Ezin, M., Shook, D. and Skoglund, P. (2000). Mechanisms of convergence and extension by cell intercalation. *Philos. Trans. R. Soc. London Ser. B* **355**, 897-922.

Krendel, M., Zenke, F. T. and Bokoch, G. M. (2002). Nucleotide exchange factor GEF-H1 mediates cross-talk between microtubules and the actin cytoskeleton. *Nat. Cell Biol.* **4**, 294-301.

Kwan, K. M. and Kirschner, M. W. (2003). Xbra functions as a switch between cell migration and convergent extension in the *Xenopus* gastrula. *Development* **130**, 1961-1972.

Lane, M. C. and Keller, R. (1997). Microtubule disruption reveals that Spemann's organizer is subdivided into two domains by the vegetal alignment zone. *Development* **124**, 895-906.

Leise, W. F., 3rd and Mueller, P. R. (2004). Inhibition of the cell cycle is required for convergent extension of the paraxial mesoderm during *Xenopus* neurulation. *Development* **131**, 1703-1715.

Marlow, F., Topczewski, J., Sepich, D. and Solnica-Krezel, L. (2002). Zebrafish Rho kinase 2 acts downstream of Wnt11 to mediate cell polarity and effective convergence and extension movements. *Curr. Biol.* **12**, 876-884.

Marsden, M. and DeSimone, D. W. (2003). Integrin-ECM interactions regulate cadherin-dependent cell adhesion and are required for convergent extension in *Xenopus*. *Curr. Biol.* **13**, 1182-1191.

Morgan, R., Hooiveld, M. H. and Durston, A. J. (1999). A novel guanine exchange factor increases the competence of early ectoderm to respond to neural induction. *Mech. Dev.* **88**, 67-72.

Nobes, C. D. and Hall, A. (1995). Rho, rac and cdc42 GTPases: regulators of actin structures, cell adhesion and motility. *Biochem. Soc. Trans.* **23**, 456-459.

Peng, H. B. (1991). *Xenopus laevis*: practical uses in cell and molecular biology. Solutions and protocols. *Methods Cell Biol.* **36**, 657-662.

Saka, Y. and Smith, J. C. (2001). Spatial and temporal patterns of cell division during early *Xenopus* embryogenesis. *Dev. Biol.* **229**, 307-318.

Shih, J. and Keller, R. (1992). Cell motility driving mediolateral intercalation in explants of *Xenopus laevis*. *Development* **116**, 901-914.

Sterpetti, P., Hack, A. A., Bashar, M. P., Park, B., Cheng, S. D., Knoll, J. H., Urano, T., Feig, L. A. and Toksoz, D. (1999). Activation of the Lbc Rho exchange factor proto-oncogene by truncation of an extended C terminus that regulates transformation and targeting. *Mol. Cell. Biol.* **19**, 1334-1345.

Tahinci, E. and Symes, K. (2003). Distinct functions of Rho and Rac are required for convergent extension during *Xenopus* gastrulation. *Dev. Biol.* **259**, 318-335.

Wallingford, J. B., Rowning, B. A., Vogeli, K. M., Rothbacher, U., Fraser, S. E. and Harland, R. M. (2000). Dishevelled controls cell polarity during *Xenopus* gastrulation. *Nature* **405**, 81-85.

Wallingford, J. B., Fraser, S. E. and Harland, R. M. (2002). Convergent extension: the molecular control of polarized cell movement during embryonic development. *Dev. Cell* **2**, 695-706.